1996ApJ...458..215H

THE ASTROPHYSICAL JOURNAL, 458:215–221, 1996 February 10
© 1996. The American Astronomical Society. All rights reserved. Printed in U.S.A.

A NEW LOOK AT CARBON ABUNDANCES IN PLANETARY NEBULAE. I. PB 6, Hu 2–1, K648, AND H4–1

R. B. C. HENRY,[1] K. B. KWITTER,[2] AND J. W. HOWARD[1]
Received 1995 May 19; accepted 1995 August 11

ABSTRACT

We introduce and describe a new long-term project whose goal is to employ final archived *IUE* spectra to study carbon abundances in a sample of planetary nebulae representing a broad range in progenitor mass and metallicity. In this paper we report on initial results for PB 6, Hu 2–1, K648, and H4–1. Our UV line strengths for H4–1 are the first such data to be published for this object. By combining our measured UV line strengths with optical line strengths found in the literature for each object, we have determined values for the abundance ratios He/H, O/H, C/O, N/O, and Ne/O using a combined atomic level-balancing-photoionization model approach. Eventually, the abundances from this and subsequent studies will be analyzed using a newly improved stellar evolution code for intermediate-mass stars with the goal of determining carbon yields for stars of this mass range.

Subject headings: ISM: abundances — planetary nebulae: general — stars: evolution

1. INTRODUCTION

Carbon production in intermediate-mass stars plays a significant role in the chemical evolution of a galaxy (Tinsley 1978). In fact, Sarmiento & Peimbert (1985) estimate that these objects contribute as much as 60%–80% of the carbon found in the interstellar medium. Thus, while the buildup of most heavier elements such as oxygen, sulfur, and silicon in galaxies is primarily controlled by massive stars, to understand the accumulation of carbon over time, we must turn to the study of intermediate-mass stars. In particular, we need to understand carbon production as a function of stellar mass and metallicity, since galactic enrichment is really controlled by an ensemble of stars representing a range in these parameters.

A major effort in regard to intermediate-mass star yields was carried out by Renzini & Voli (1981), who computed detailed stellar evolution models over a relevant mass range in an attempt to interpret planetary nebula (PN) and carbon star abundances in terms of stellar yields. Indeed, it is the Renzini & Voli nucleosynthesis prescriptions which are usually employed in galactic chemical evolution computations such as those for the galactic disk by Matteucci & François (1989). Since Renzini & Voli's work, however, more *IUE* spectral data for PNs have become available, and with the advent of final archived data, in which raw *IUE* spectra collected over the satellite's lifetime are being reduced in a consistent fashion, it is now possible for the first time to obtain a homogeneous set of UV line strengths for a broad sample of PNs. This will allow a determination of carbon abundances in which systematic errors due to data reduction are minimized. In addition, important changes in theory such as better opacities, an improved core-mass/luminosity relation, and advances in dredge-up theory now make the Renzini & Voli models obsolete. Therefore, the subject of carbon production in intermediate-mass stars needs to be revisited.

The purpose of this paper is to provide an introduction and progress report on a project whose long-range goal is to reanalyze optical and final archived *IUE* data in order to determine chemical abundances of several elements, including (especially) carbon in PNs. A major second step will be to employ a detailed stellar evolution code to infer progenitor star properties from our abundance results for a sample of PNs chosen to span the range of progenitor star masses. A complete list of our sample PNs, including type designation, is presented in Table 1. We point out that our study is complementary to the large one carried out recently by Rola & Stasińska (1994) in that we focus on a smaller sample but attempt to model each nebula.

We report here on the results from the analysis of four PNs from Table 1. These objects were selected because of their small angular size in order to avoid initially the problem of linking UV and optical spectra when different aperture sizes are employed. The four planetaries, PB 6, Hu 2–1, K648, and H4–1 represent a broad range in progenitor star mass and metallicity; where PB 6 is a nitrogen-rich type I object and presumably the product of a massive progenitor, Hu 2–1 is a type II/III object, and K648 and H4–1 are both halo PNs representing progenitor stars of relatively low mass and metallicity.

For each of these objects, we have obtained and measured all available *IUE* spectra which have been rereduced as part of the *IUE* final archiving program. The UV spectral data were then linked with optical spectra in the literature, and chemical abundances of carbon and other elements as well as central star properties were inferred using an analysis technique involving both empirical and photoionization modeling methods.

A description of the final archive program and the UV data for the first four objects in our sample are given in § 2. In § 3 we describe our analysis procedure and present our results, and we summarize our findings in § 4.

2. THE DATA

Ultraviolet line strengths of C III] λ1909, C IV λ1549, and other lines of interest to this program were measured with routines in IRAF using newly reduced and flux-calibrated

[1] Department of Physics and Astronomy, University of Oklahoma, Norman, OK 73019; henry@phyast.nhn.uoknor.edu; howard@phyast.nhn.uoknor.edu.
[2] Department of Astronomy, Williams College, Williamstown, MA 01267; karen.b.kwitter@williams.edu.

© American Astronomical Society • Provided by the NASA Astrophysics Data System

1996ApJ...458..215H

TABLE 1

PROGRAM PLANETARY NEBULAE

Object	Type
BB–1	Halo
DDDM-1	Halo
Hu 2–1	II–III
H4–1	Halo
IC 3568	II–III
IC 418	I
IC 4593	I
K648	Halo
IC 1535	II–III
NGC 2392	I
NGC 2440	I
NGC 3241	II–III
NGC 650	I
NGC 6210	II–III
NGC 6720	II–III
NGC 6826	II–III
NGC 7009	II–III
NGC 7027	II
NGC 7293	I
PB 6	I
PN 06–41.1	Halo
YM 29	I

SWP spectra available in the final archive of the *IUE* database. The final archive program was begun nearly 2 yr ago with the goals of (1) producing a uniformly processed and calibrated archive of all of the *IUE* data, and (2) exploiting new image processing techniques developed during the mission which improve both the photometric accuracy and signal-to-noise ratio of the data. These improvements have been made possible by the use of a weighted slit extraction method and the use of white dwarf models for carrying out the flux calibrations. In the end, spectral resolution has been improved and the signal-to-noise ratio has been increased by 10%–50%. Table 2 lists the *IUE* spectra measured for each of the four PNs in our current study, along with the exposure times, and Figure 1 shows the final archived spectrum SWP 36242 for PB 6 as an example of the data with which we are working. All spectra analyzed in this study were obtained through the large *IUE* aperture (21″.7 × 9″.1; *IUE* NEWSIPS Manual, 1993). The raw UV line strengths for each object were corrected for interstellar reddening using the extinction curve from Seaton (1979). The logarithmic extinction quantity c was determined from optical data for the same object taken from the literature.

TABLE 2

FINAL ARCHIVE SPECTRA

Object	SWP	Exposure Time (s)
PB 6	29857	24000
	30147	05400
	36238	10800
	36242	03600
Hu 2–1	03659	02400
	06642	01200
	08589	02400
K648	07233	03000
	08786	08520
	09240	03600
	09261	10800
	09580	02700
	09605	01200
	17069	03600
H4–1	07220	07080
	14410	00900
	14411	02220
	20599	03600

It is now necessary to join UV with optical line strengths from the literature so that abundance studies can be carried out. However, accurate linking of UV and optical spectra is

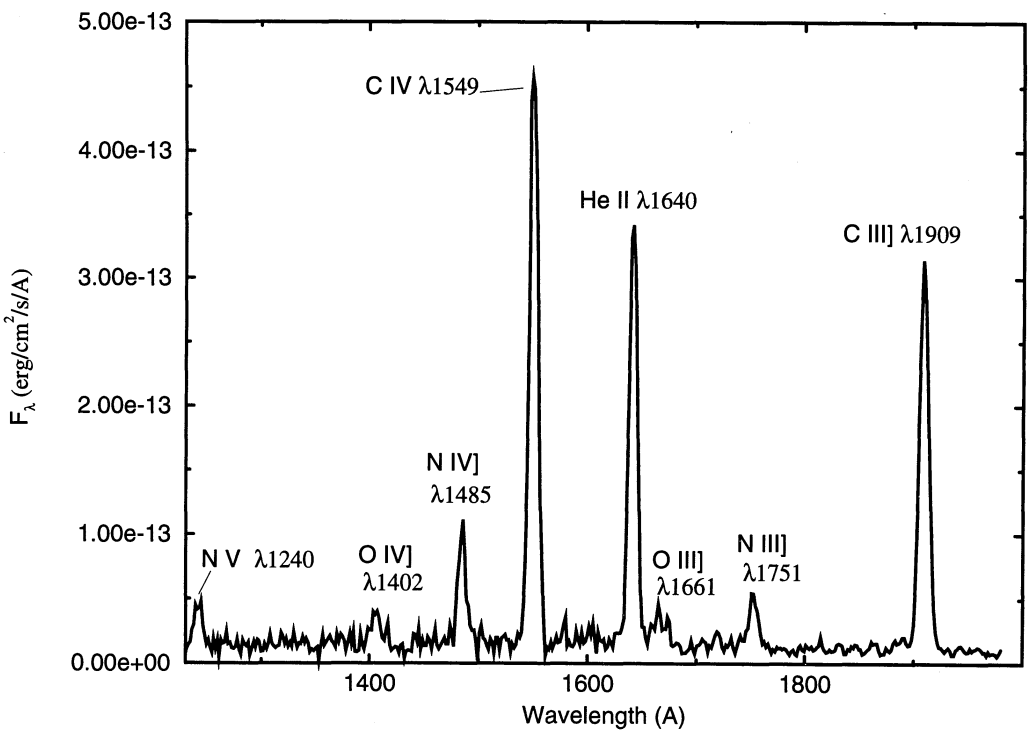

FIG. 1.—*IUE* final archived spectrum SWP 36242 of PB 6, with important emission lines indicated

© American Astronomical Society • Provided by the NASA Astrophysics Data System

1996ApJ...458..215H

complicated in the absence of any spectral overlap and/or a noncorrespondence between the sizes and positions of the spectrograph slits for the UV and optical observations. In the first instance, systematic differences in flux calibrations on two different systems threaten accurate alignment of the two spectral regions. In the second instance, the two spectra may actually include different parts of the nebula. By limiting our present sample to objects of small angular size we have for now avoided the second problem, although the absence of spectral overlap is still a problem for all four objects. This situation can be remedied for the most part by employing a line ratio whose value is relatively insensitive to physical conditions in the nebula and the lines fall in the two different spectral regions. The intensity ratio He II λ1640/λ4686 is useful in this instance, and theoretically predicted values found in Hummer & Storey (1987) for different gas densities and temperatures were used to scale the observed UV intensities to published optical line strengths in the cases of PB 6 and H4–1, objects in which both He II lines were measured. For PB 6, we assumed a He II line ratio of 7.04, while a value of 6.72 was used for H4–1. For Hu 2–1 and K648, He II λ1640 was not detected in the UV; thus the alignment of UV and optical spectra relied solely on the published fluxes for the latter.

Table 3 lists our UV fluxes and reddening-corrected intensities as measured using *IUE* final archived spectra for our four sample objects. For each line listed in column (1), the reddening coefficient f is provided in column (2), followed in alternating fashion by observed fluxes and corrected intensities normalized to Hβ = 100. For those cases in which an emission line could be measured in more than one spectrum for the same object, the adopted line strength represents an average of individual values weighted by the square root of the integration time. The last three rows of Table 3 give logarithmic Hβ fluxes, the logarithmic extinction quantity c, and the references for the optical data used for each object.

The quality of each emission line was evaluated with regard to saturation and other possible defects, using data stored for this purpose with each spectrum, and heavily compromised features were ignored. Uncertainties in UV line fluxes given in parentheses following each value in Table 3 are derived from rms noise measurements as well as uncertainties in the Hβ flux and the extinction coefficient c, all added together in quadrature. The noise contribution was determined from rms continuum measurements made near each spectral feature in each spectrum contributing to a line strength determination.

Fluxes for optical emission features (uncorrected for reddening) to be used in the abundance study below were taken from the sources listed in the last row of Table 3. The optical line strengths were corrected for reddening using Savage & Mathis's (1979) extinction curve. In the case of H4–1, we used the value of $F_{H\beta}$ from Hawley & Miller (1978), but the relative optical line strengths were taken from Torres-Peimbert & Peimbert (1979).

Finally, we note that the UV line strengths for H4–1 in Table 3 represent the first time that UV data have been published for this object. In Figure 2 we present the final archived spectrum SWP 20599, which is a 1 hr integration on H4–1. Prominent emission features are marked.

3. RESULTS

3.1. *Abundance Calculations*

We have determined the abundance ratios by number of He/H, O/H, C/O, N/O, and Ne/O for the four PNs from the UV and optical line strengths described in § 2. We make use of an updated version of ABUN, a level-balancing program first used by Henry (1990) which takes observed line intensities as input and returns abundance ratios as well as electron temperatures and densities as output. We also use the photoionization code CLOUDY (Ferland 1990) to construct a consistent model of the nebula in order to further correct abundances derived using ABUN. The process flows as follows for each object being studied.

1. ABUN is used to get a preliminary set of abundance ratios $A^{PN}_{abun}(X)$, where X is one of the ratios above;
2. CLOUDY is used to produce a photoionization model which closely matches the observed values for four important

TABLE 3

UV LINE STRENGTHS[a]

		PB 6		Hu 2–1		K648		H4–1	
LINE (1)	$f(\lambda)$ (2)	$F(\lambda)$ (3)	$I(\lambda)$[b] (4)	$F(\lambda)$ (5)	$I(\lambda)$ (6)	$F(\lambda)$ (7)	$I(\lambda)$ (8)	$F(\lambda)$ (9)	$I(\lambda)$[c] (10)
C III λ1175	1.85	...	...	...	...	...	...	45(±48)	52(±64)
N V λ1240	1.64	23(±5)	215(±49)	...	...	6(±3)	7(±5)	...	...
C II λ1336	1.41	...	...	...	...	...	...	45(±23)	48(±33)
O IV] λ1402	1.31	13(±1)	85(±8)	...	...	...	...	...	...
N IV] λ1485	1.23	53(±5)	321(±33)	...	...	...	...	...	...
C IV λ1549	1.18	290(±15)	1659(±106)	...	...	...	...	134(±52)	138(±74)
He II λ1640	1.14	196(±14)	1073(±86)	...	...	...	...	64(±30)	65(±39)
O III] λ1661	1.13	6(±3)	32(±16)	...	...	...	...	...	...
N III] λ1751	1.12	20(±6)	107(±32)	...	...	8(±3)	9(±5)	...	...
C III] λ1909	1.23	207(±11)	1251(±83)	13(±5)	44(±17)	326(±24)	382(±137)	449(±117)	465(±212)
log $F_{H\beta}$[d]		−11.87(±0.02)		−10.82(±0.02)		−12.15(±0.03)		−12.58(±0.10)	
c			0.481(±0.014)		0.437(±0.014)		0.056(±0.124)		0.072(±0.124)
References[e]		K		B		A		H, T	

[a] Normalized to Hβ = 100.
[b] Values scaled so that He II λ1640/He II λ4686 = 7.04 (Hummer & Storey 1987).
[c] Values scaled so that He II λ1640/He II λ4686 = 6.72 (Hummer & Storey 1987).
[d] Erg cm^{-2} s^{-1}.
[e] K = Kaler et al. 1991; B = Barker 1978a; A = Adams et al. 1984; H = Hawley & Miller 1978; T = Torres-Peimbert & Peimbert 1979.

© American Astronomical Society • Provided by the NASA Astrophysics Data System

1996ApJ...458..215H

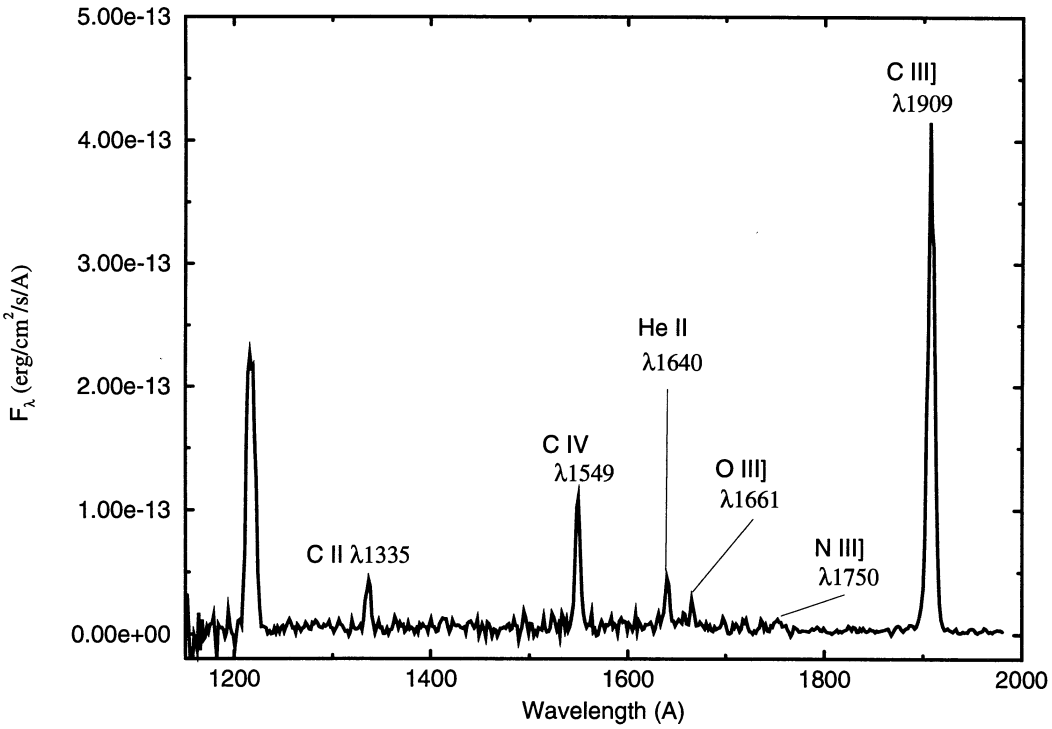

FIG. 2.—*IUE* final archived spectrum SWP 20599 of H4–1. The integration time is 3600 s. Important emission lines are shown

diagnosics involving the strengths of the following emission lines in the manner shown:
(a) [O II] λ3727 + [O III] λλ4959, 5007/Hβ; (b) [O III] λ4363/[O III] λ5007; (c) [S II] λ6716/λ6731; and (d) [O II] λ3727/[O III] λλ4959, 5007.
We designate the model input abundance ratios as $A_{\rm in}^{\rm mod}(X)$;

3. ABUN is then used along with model output emission line intensities to obtain abundance ratios $A_{\rm abun}^{\rm mod}(X)$;

4. Final abundance ratios $A_F^{\rm PN}(X)$ are then obtained by assuming that:

$$A_F^{\rm PN}(X) = A_{\rm abun}^{\rm PN}(X)\xi(X)\,, \tag{1a}$$

where

$$\xi(X) = \frac{A_{\rm in}^{\rm mod}(X)}{A_{\rm abun}^{\rm mod}(X)}\,. \tag{1b}$$

Note that this scheme is similar to the one employed by Shields et al. (1981) and Aller & Czyzak (1983). However, instead of deriving ionization correction factors from the models in order to go from ionic to elemental abundances as they did, we use the models to derive ξ, the ratio of input abundances to those inferred using ABUN on the model output spectrum. We then make the assumption that the ξ is also equal to the ratio of actual abundances to those inferred using ABUN in the real PNs.

Abundance ratios are calculated by ABUN using the following relations between ionic and elemental abundances:

$$\frac{\rm He}{\rm H} = \frac{{\rm He}^+ + {\rm He}^{+2}}{{\rm H}^+}\,, \tag{2a}$$

$$\frac{\rm O}{\rm H} = \frac{{\rm O}^+ + {\rm O}^{+2}}{{\rm H}^+}\cdot\frac{{\rm He}^+ + {\rm He}^{+2}}{{\rm He}^+}\,, \tag{2b}$$

$$\frac{\rm N}{\rm O} = \frac{{\rm N}^+}{{\rm O}^+}\,, \tag{2c}$$

$$\frac{\rm C}{\rm O} = \frac{{\rm C}^{+2}}{{\rm O}^{+2}}\,, \tag{2d}$$

$$\frac{\rm Ne}{\rm O} = \frac{{\rm Ne}^{+2}}{{\rm O}^{+2}}\,. \tag{2e}$$

Emission lines used for calculating the abundance ratios are He I λ5876, He II λ4686, [O II] λ3727, [O III] λ5007, [N II] λ6584, [C III] λ1909, and [Ne III] λ3869, where the line strengths with respect to Hβ are entered into ABUN. Sources for atomic data used in these calculations are given in Table 4.

Equation (2d) was shown to be valid by Rola & Stasińska (1994) in their study of carbon abundances in PNs (see their Fig. 6). We have further checked out this relation using our

TABLE 4

ABUN: SOURCES OF ATOMIC DATA

Ion	Data Type[a]	Reference
H^0.....	$\alpha_{\rm eff}(\lambda4861)$	Brocklehurst 1971
He^0	$\alpha_{\rm eff}(\lambda5876)$[b]	Seaton 1968; Robbins 1968
He^+	$\alpha_{\rm eff}(\lambda4686)$	Brocklehurst 1971
O^+	Ω	Mendoza 1983
	A	Zeippen 1987
O^{+2}.....	Ω	Mendoza 1983
	A	Mendoza 1983
N^+	Ω	Mendoza 1983
	A	Mendoza 1983
C^{+2}	Ω	Mendoza 1983
	A	Berrington et al. 1985
Ne^{+2}.....	Ω	Butler & Mendoza 1984
	A	Mendoza 1983

[a] $\alpha_{\rm eff}$ = effective recombination coefficient; Ω = collision strengths; A = transition rates.
[b] Includes collisional effects given by Clegg 1987.

© American Astronomical Society • Provided by the NASA Astrophysics Data System

1996ApJ...458..215H

TABLE 5A

OBSERVATIONS AND MODELS[a]

	PB 6		Hu 2–1		K648		H4–1	
PARAMETER	Observations	Model	Observations	Model	Observations	Model	Observations	Model
$\log (I_{[O\,II]} + I_{[O\,III]})/H\beta$	+1.14	+1.18	+0.81	+0.88	+0.49	+0.49	+1.09	+1.05
$\log I_{[O\,II]}/I_{[O\,III]}$	−1.27	−1.27	−0.71	−0.69	−1.02	−1.03	−0.69	−0.55
$\log I_{\lambda 4363}/I_{\lambda 5007}$	−1.68	−1.71	−2.45	−2.23	−1.89	−1.89	−1.96	−1.70
$\log I_{\lambda 6716}/I_{\lambda 6731}$	−0.18	−0.16	−0.18	−0.18	...	−0.05	0.00	−0.04
T_{eff} (10^3 K)		150		40		45.6		132
$\log U$		−1.90		−1.55		−1.65		−2.92
N_e		2800		2800		1000		1100
[He/H]		0.00		0.00		−0.03		+0.09
[O/H]		−0.60		−0.52		−1.32		−0.87
[C/O]		+0.60		+0.70		+1.26		0.10
[N/O]		+0.78		+0.30		−0.01		+0.32
[Ne/O]		0.00		−0.10		−0.20		−0.96
[S/O]		0.00		0.00		+0.22		−0.75

[a] Model abundances are expressed logarithmically and normalized to solar values.

TABLE 5B

COMPARISON OF CENTRAL STAR TEMPERATURES AND NEBULAR DENSITIES

	PB 6		Hu 2–1		K648		H4–1	
PARAMETER	Current	Other	Current	Other	Current	Other	Current	Other
T_* (10^3 K)	150	103	40	38.0	45.6	38.0	132	83.2
N_e (10^3 cm^{-3})	2.8	2.1	2.8	13.0	1.0	1.7	1.1	0.8
References[a]		K		KM, B		A		KM, T

REFERENCES.—K = Kaler et al. 1991; B = Barker 1978a; A = Adams et al. 1984; KM = Kohoutek & Martin 1981; T = Torres-Peimbert & Peimbert (1979).

TABLE 5C

CORRECTION FACTORS (ξ)

Ratio	PB 6	Hu 2–1	K648	H4–1
He/H	1.12	1.00	0.93	1.00
O/H	1.05	0.89	0.93	0.91
C/O	1.45	0.88	0.98	0.95
N/O	1.16	1.47	1.38	0.89
Ne/O	0.87	0.95	0.93	0.74

own grid of photoionization models spanning a wide range of physical conditions. For each model we calculated ξ for C/O and found values ranging between 1 and 2, where the largest deviations ($\sim$2) occur in model nebulae with relatively cool (T_{eff} = 50,000 K) central star temperatures, in good agreement with the findings of Rola & Stasińska. Thus, our method for obtaining C/O appears to be quite reliable for PNs, as will be shown below for the specific objects treated here.

Table 5A contains the results of steps 1 and 2 of our procedure, where the close agreement between model and observations for each object is evident for the diagnostic ratios in the first four rows. The last nine rows list model input parameters; note that the abundance ratios listed are logarithmic values normalized to their solar levels as given in Grevesse & Anders (1989).

Table 5B compares our derived (current) central star temperatures and nebular densities with values from the other studies referenced. (Abundance comparisons are made below.) Overall, our results are consistent with previous work. There is a sizable discrepancy between our derived nebular density for Hu 2–1 and Barker's (1978a) result for the same object. In addition, our stellar temperatures for PB 6 and H4–1 differ somewhat from earlier values. The temperature discrepancy may be due to the fact that our values are blackbody effective temperatures which are chosen because they produce models results consistent with observations, while the temperatures from the literature in these two cases are Zanstra temperatures.

Table 5C lists the abundance correction factors, $\xi(X)$, as determined in steps 2 and 3. Since a value of unity corresponds to a perfect match between input and output abundances, one can see that ABUN derives abundances always within about 50% of the input levels. These relatively small deviations attest to the effectiveness of all relations in equations (2a)–(2e) for the objects being investigated here.

3.2. *Derived Abundances*

Our final abundances are given in Table 6, where we also list solar values from Grevesse & Anders (1989) in the last column. Percent uncertainties, estimated from line strength uncertainties for UV (Table 3) and optical features in all but PB 6 are given beneath the derived value for each abundance ratio. Uncertainties for PB 6 are not available for the Kaler et al. (1991) observations.

The abundances reported in Table 6 represent the endpoint of the four-step procedure described above. Figure 3 is a plot of these ratios presented logarithmically and normalized to the respective solar ratio for each of the four objects studied here. Solid symbols refer to abundances derived in this paper, while open symbols are results from other authors, as indicated in the figure caption. Error bars show the estimated uncertainties from Table 6.

© American Astronomical Society • Provided by the NASA Astrophysics Data System

1996ApJ...458..215H

TABLE 6

DERIVED ABUNDANCES

RATIO	OBJECTS				
	PB 6	Hu 2–1	K648	H4–1	Sun[a]
He/H.....	0.20	0.11	8.30(−2)	0.10	9.80(−2)
±%	...	15	25	10	
O/H.....	6.29(−4)	3.11(−4)	4.12(−5)	2.15(−4)	8.51(−4)
±%	...	10	20	10	
C/O	2.67	1.79	4.68	1.91	0.43
±%	...	40	40	15	
N/O.....	0.43	0.38	0.11	0.23	0.13
±%	...	10	30	15	
Ne/O.....	0.18	0.11	0.07	1.10(−2)	0.14
±%	...	10	30	15	

[a] Grevesse & Anders 1989.

As demonstrated in Figure 3, our abundances are reasonably consistent with those previously determined by others with the exceptions of N/O for PB 6 and Hu 2–1. In addition, our C/O values are systematically lower than earlier published results. Evidently this is not due to differences in line strengths between previous and final archived *IUE* data, as a comparison indicates earlier measurements are consistent with our current ones. However, we plan to *compare* final archived with originally published data more extensively after UV measurements of more of our program objects have been made from the final archive database.

Our sample of four objects include a type I (PB 6), a type II-III (Hu 2–1), and two halo PNs (K648 and H4–1). Metallicity generally decreases along the sequence type I, type II, type III, halo. Note that our derived oxygen abundances are consistent with this pattern. The He abundance of PB 6 is shown to be unusually high, at over twice solar. We note that the strength of He II λ4686 in PB 6 measured by Kaler et al. (1991) is uncharacteristically high for a gaseous nebula; it is primarily this line which is causing the inferred He abundance to be so large. Additional measurements of this line in PB 6 are needed to confirm that the He abundance is truly at the level indicated here. We also see in Figure 3 that K648 has an unusually high abundance of carbon relative to nitrogen and oxygen, perhaps suggesting that significantly less nitrogen production through the CN cycle has occurred.

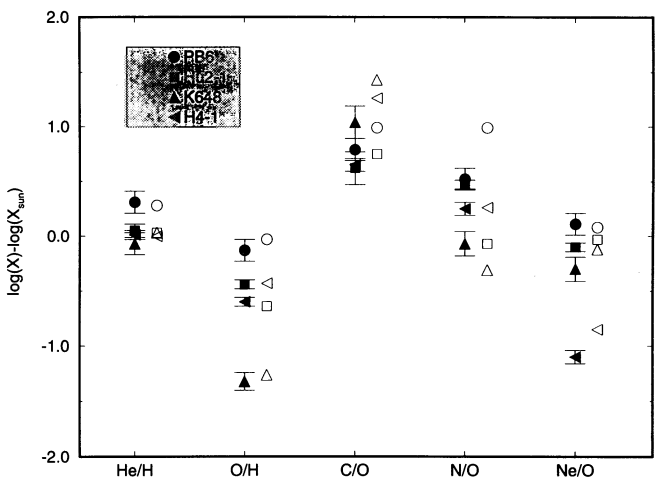

FIG. 3.—Derived abundance ratios for four objects studied here. Values on the vertical axis are normalized to solar using data from Grevesse & Anders (1989) and are presented logarithmically, where X corresponds to one of the ratios shown along the horizontal axis. Filled symbols are our results. Open symbols show abundances published previously by Kaler et al. (1991; PB 6); Barker (1978b; Hu 2–1); Lutz (1981; Hu 2–1); Adams et al. (1984; K648); Barker (1983; K648, H4–1), and Torres-Peimbert & Peimbert (1979; H4–1).

Taken together, the abundances for the four PNs show *significantly enhanced* carbon and nitrogen (except for K648) with respect to oxygen and *depleted* oxygen, all relative to the Sun. The enhancements are presumably the result of the dredge-up of nucleosynthetic products during progenitor star evolution, while the oxygen depletion may arise from two separate causes: for PB 6, a type I PN with a massive (probably) progenitor, significant ON cycling during the star's evolution might explain the low O/H value in this object; the low O/H level in the other three objects may be related to the greater progenitor ages, and thus their formation out of metal-poor material. Further interpretation regarding abundances must await the analysis of more of our sample objects.

Finally, in deriving our abundances we have ignored possible effects of temperature fluctuations (Peimbert 1967). Such fluctuations are not expected to greatly affect ratios such as C/O, N/O, and Ne/O which are derived from ratios of collisionally excited lines. However, the determination of O/H involves both collisionally excited and recombination lines, and thus this ratio is particularly prone to temperature fluctuation effects under certain conditions. In all but PB 6, this problem is not expected to be significant. However, PB 6 is a type I object, and these PNs are usually characterized by filaments and clumps where temperature fluctuations are more likely. Thus, our value for O/H in PB 6 must be viewed with this qualification in mind, while we are confident that all other abundance ratios are relatively unaffected by temperature fluctuations.

4. SUMMARY

We have begun a long-term project whose goal is to study the production of carbon in intermediate-mass stars. In the current paper, we report on the use of low-dispersion SWP spectra from the recently established *IUE* final archive to measure lines of C III] λ1909, C IV λ1549, He II λ1640, and other features observed in four PNs representing a range in progenitor mass and metallicity. We have combined these measurements with optical line strengths in the literature to calculate abundances of helium, carbon, nitrogen, oxygen, and neon. Our technique combines level-balancing computations with photoionization models which are calculated to match four important nebular diagnostic ratios. For this, our first use of the procedure described within, we chose four PNs of small angular size to avoid as much as possible any problems related to slit size and positioning differences arising from the separate UV and optical data acquisition.

We find abundances which are for the most part consistent with past results for these objects in the literature. Specifically, we find that relative to the Sun all four objects show enhanced C/O but depleted O/H, while three of the four show enhanced N/O. All three trends are qualitatively consistent with stellar nucleosynthesis theories for intermediate-mass stars and the ages of the progenitor stars as inferred from their Peimbert types.

This project is supported by NASA grant NAG 5-2389. We would like to thank C. Imhoff, J. Nichols, and R. Thompson at NASA/GSFC for their helpful assistance during the develop-

© American Astronomical Society • Provided by the NASA Astrophysics Data System

1996ApJ...458..215H

ment and execution of this project. In addition, we are grateful to M. Peimbert for valuable discussions concerning the problem of temperature fluctuations. Finally, R. B. C. H. would like to express his appreciation to members of the Astronomy Department at Williams College for the warm hospitality accorded him during several productive visits.

REFERENCES

Adams, S., Seaton, M. J., Howarth, I. D., Aurière, M., & Walsh, J. R. 1984, MNRAS, 207, 471
Aller, L. H., & Czyzak, S. J. 1983, ApJS, 51, 211
Barker, T. 1978a, ApJ, 219, 914
———. 1978b, ApJ, 220, 193
———. 1983, ApJ, 270, 641
Berrington, K. A., Burke, P. G., Dufton, P. L., & Kingston, A. E. 1985, Atomic Nuclear Data, 33, 195
Brocklehurst, M. 1971, MNRAS, 153, 471
Butler, K., & Mendoza, C. 1984, MNRAS, 208, 17P
Clegg, R. E. S. 1987, MNRAS, 229, 31P
Ferland, G. J. 1990, Ohio State Univ. Rep. 90–02
Grevesse, N., & Anders, E. 1989, in Cosmic Abundances of Matter (AIP Conf. Proc. 183), ed. C. J. Waddington
Hawley, S. A., & Miller, J. S. 1978, ApJ, 220, 609
Henry, R. B. C. 1990, ApJ, 356, 229
Hummer, D. G., & Storey, P. J. 1987, MNRAS, 224, 801
Kaler, J. B., Shaw, R. A., Feibelman, W. A., & Imhoff, C. L. 1991, PASP, 103, 67
Kohoutek, L., & Martin, W. 1981, A&A, 94, 365
Lutz, J. H. 1981, ApJ, 247, 144
Matteucci, F., & François, P. 1989, MNRAS, 239, 885
Mendoza, C. 1983, IAU Symp. 103, Planetary Nebulae, ed. D. R. Flower (Dordrecht: Reidel), 143
Peimbert, M. 1967, ApJ, 150, 825
Renzini, A., & Voli, M. 1981, A&A, 94, 175
Robbins, R. R. 1968, ApJ, 151, 497
Rola, C., & Stasińska, G. 1994, A&A, 282, 199
Sarmiento, A., & Peimbert, M. 1985, Rev. Mexicana Astron. Af., 11, 73
Savage, B. D., & Mathis, J. S. 1979, ARA&A, 17, 73
Seaton, M. J. 1968, in IAU Symp 34, Planetary Nebulae, ed. D. E. Osterbrock & C. R. O'Dell (Dordrecht: Reidel), 131
Seaton, M. J. 1979, MNRAS, 187, 73P
Shields, G. A., Aller, L. H., Keyes, C. D., & Czyzak, S. J. 1981, ApJ, 248, 569
Tinsley, B. M. 1978, in IAU Symp. 76, Planetary Nebulae (Dordrecht: Reidel), 341
Torres-Peimbert, S., & Peimbert, M. 1979, Rev. Mexicana Astron. Af., 4, 341
Zeippen, C. J. 1987, A&Ap, 173, 410

© American Astronomical Society • Provided by the NASA Astrophysics Data System